Available online at www.sciencedirect.com
SCIENCE DIRECT
Lithos 79 (2005) 25–41
LITHOS
www.elsevier.com/locate/lithos

Partial melting of slab window margins: genesis of adakitic and non-adakitic magmas

Derek J. Thorkelson[a,*], Katrin Breitsprecher[b]

[a]*Department of Earth Sciences, Simon Fraser University, Burnaby, British Columbia, Canada, V5A 1S6*
[b]*Department of Earth and Ocean Sciences, University of British Columbia, Vancouver, British Columbia, Canada, V6T 1Z4*

Received 8 October 2003; accepted 2 September 2004
Available online 2 November 2004

Abstract

When a mid-ocean spreading ridge subducts, it typically splits apart at depth to form two tapered slab edges separated by asthenospheric mantle within a slab window. We examine the fate of the slab edges using simplified slab window geometries, specific thermal parameters, and assumptions regarding shear stress and slab hydration. Six fundamental zones of slab anatexis are identified and classified according to expected melt and restite compositions. Non-adakitic melts of granodioritic to tonalitic composition are generated along the plate edges at depths of 5–65 km, whereas adakitic melts form proximal to the edges at depths of 25–90 km. As anatexis proceeds, the subducted crust is converted to a migmatite of slab melt and eclogitic restite. Much of the migmatite may shear away from the slab and become incorporated into the mantle. The melts will rise and leave behind fragments of restite within mantle peridotite. If the peridotite is part of the overriding plate, then the restite fragments may become long-term residents of the continental lithospheric mantle. However, if the restite becomes entrained in the asthenosphere, it may undergo upwelling and melting, or flow away as ductile streaks to become long-term mantle heterogeneities. Slab windows are thereby identified as important sites for slab melting and geochemical replenishment of the mantle.

Keywords: Slab window; Ridge subduction; Adakite; Anatexis; Mantle; Restite

1. Introduction

Ridge subduction and concomitant slab window formation are principal causes of igneous, metamorphic and structural variations in active continental margins (Dickinson and Snyder, 1979; Johnson and O'Neil, 1984; Forsythe and Nelson, 1985; Thorkelson and Taylor, 1989; Sisson et al., 1994; Thorkelson, 1996; Sisson et al., 2003). These variations are imposed on the leading edge of an overriding plate which normally consists of an amagmatic forearc, an active volcanic arc, and a back-arc which may or may not be magmatically active. When a ridge is subducted, the forearc tends to become heated, intruded by magmas, and deformed (Marshak and

* Corresponding author. Tel.: +1 604 291 5390; fax: +1 604 291 4198.
E-mail addresses: dthorkel@sfu.ca (D.J. Thorkelson), kbreitsp@eos.ubc.ca (K. Breitsprecher).

0024-4937/$ - see front matter © 2004 Elsevier B.V. All rights reserved.
doi:10.1016/j.lithos.2004.04.049

Karig, 1977; DeLong et al., 1979; Sisson and Pavlis, 1993; Groome et al., 2003); the arc tends to be extinguished or invaded by magmas of anomalous composition (Forsythe and Nelson, 1985; Hole et al., 1991; Cole and Basu, 1995; Thorkelson, 1996); and the back-arc may become more magmatically active (Gorring et al., 1997; D'Orazio et al., 2001). These various responses are driven largely by physical, thermal and chemical changes to both the underlying mantle and the subducting oceanic slabs (Delong et al., 1979; Benz et al., 1992; Hole and Larter, 1993; Lewis et al., 1997). For example, the slab is progressively younger and hotter toward the subducting ridge, and the mantle within the slab window will tend to be hotter and less hydrated (Thorkelson, 1996; Sisson et al., 2003). These changes to the subduction environment are, in turn, affected by a range of dynamic processes. For example, upwelling or lateral flowage of asthenosphere will lead to displacement of the mantle wedge with peridotite of different chemical and thermal characteristics (Johnston and Thorkelson, 1997; Murdie and Russo, 1999; Frederiksen et al., 1998); thermal erosion of slab window margins (Severinghaus and Atwater, 1990) will liberate slab-anatectic melts and contaminate the ambient mantle (Thorkelson, 1996); and migration of the ridge–trench intersection will tend to produce diachroneity of the aforementioned effects in the overriding plate (Johnson and O'Neil, 1984; Gorring et al., 1997; Thorkelson and Taylor, 1989; Haeussler et al., 2003). Consequently, the igneous responses to a migrating slab window are both compositionally complex and time-transgressive.

In this paper, we focus on the genesis of slab melts derived from thermal erosion of slab window margins, specifically the anatexis of subducted igneous crust. Our work brings together established phase equilibria, *P*–*T* paths of subducting slabs, and physical models of ridge subduction to provide the first detailed identification of slab-melt regions in slab window environments. This investigation is carried out using idealized slab window geometries constructed using the structural principles of Thorkelson (1996). The topics of melt transport and emplacement, and the various factors governing compositional variabilities in arc magmas, remain important issues in the study of slab melts. However, in this paper, we are chiefly concerned with magmagenesis rather than melt migration and modification, and we therefore focus our attention on the physical, thermal and chemical factors which influence anatexis of subducted crust.

A slab window is an asthenosphere-filled gap that forms between a pair of diverging, subducting oceanic plates in response to ridge subduction. As a spreading ridge descends into the mantle, the oceanic slabs on either side continue to diverge but cease to grow, and the ridge progressively unzips to form a gap called a slab window. Typically, ridge systems consist of ridge segments separated by transform faults, and the subduction of these different parts yield two different types of slab window margins (Fig. 1). Ridge segments widen upon subduction to form margins which taper into feather edges, reflecting the lithospheric profile acquired during sea-floor spreading (Stein and Stein, 1996); these edges are the hottest, youngest parts of the subducting slab. Transform faults, on the other hand, continue to be active as the descending plates slide past one another, during which they progressively expose square-ended slab edges. In some cases, such as at a ridge–trench–transform triple junction, only one of the oceanic plates will subduct. Additional geophysical complexities can arise if the edges of the subducting plates break up into microplates (Dickinson, 1997).

The feather edges bounding a slab window (those derived from subducting ridge segments) are more

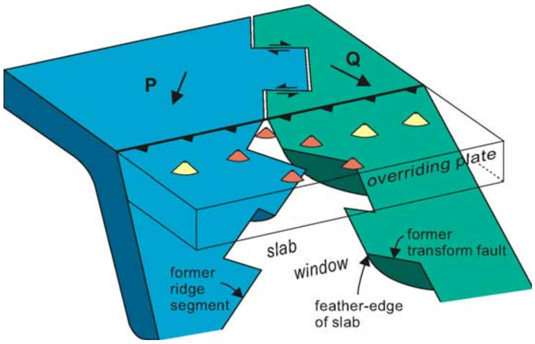

Fig. 1. Simplified slab window caused by subduction of a spreading ridge segmented by transform faults. Overriding plate is shown transparent. Motion vectors of oceanic plates P and Q are relative to the overriding plate (transparent). Slab P dips at 50° whereas slab Q dips at 25°. Volcanic arc (yellow volcanoes) is interrupted by field of anomalous magmatism (orange volcanoes) which includes products of slab anatexis. Note the feather edge morphology of subducted ridge segments. (For interpretation of the references to colour in this figure legend, the reader is referred to the web version of this article).

prone to thermal equilibration with the surrounding mantle, and more likely to undergo partial fusion, than square-ended ones (former transform faults) because of their higher surface-area to volume ratio. For this reason, we demonstrate our understanding of slab anatexis using simple slab window geometries derived from long, uninterrupted spreading ridges (i.e., without intervening transform faults). Modifications to these simplified forms can be easily made (Thorkelson, 1996), but they unnecessarily complicate the analysis and hinder the establishment of basic principles of slab antexis. Nevertheless, the general outcome of our analysis should provide an improved basis for considering partial melting along subducted transform faults which are exposed either as parts of a subducting ridge system (Fig. 1), or where a single oceanic plate is segmented into slabs of differing dip along a reactivated fracture system.

2. Magmatism in slab window environments

Magmatic effects of slab windows are varied, and explicable through several different processes. In Fig. 1, we show how "normal" arc volcanism is interrupted in the vicinity of the slab window, and replaced by a broader but possibly less voluminous volcanic field of wide-ranging compositions, including those indicative of slab anatexis. Near the trench, where the subducting ridge crest is beginning to separate, passive asthenospheric upwelling is focused across a narrow gap beneath the forearc. As mantle rises, it melts decompressively and mid-ocean ridge basalt (MORB)-like basaltic melts rise into the forearc. This process, called the blow-torch effect by DeLong et al. (1979), may trigger melting of the forearc crust to form intermediate to felsic magmas (Haeussler et al., 1995). As such, the forearc may host magmas of both MORB and granitoid compositions, particularly of peraluminous composition (Groome et al., 2003). These compositions differ from those normally found in continental margin arcs, i.e., calc-alkaline basalts and metaluminous granitoids. Farther inboard from the trench, in arc to back-arc locations, mantle upwelling through the slab window is more diffuse, being spread over a greater area than it is beneath the forearc, and results in smaller degrees of mantle melting to produce more alkalic magmas, including those with ocean–island-type (within-plate) compositions (Hole et al., 1991; D'Orazio et al., 2001; Gorring et al., 1997). Upwelling may also lead to complex thermal and chemical interaction of sub-slab asthenosphere with cooler, more hydrated peridotite in the mantle wedge, leading to mixed alkalic–calcalkalic magmas (Thorkelson, 1996; Breitsprecher et al., 2003). Advective heating from upward mantle flow can also trigger melting of ancient lithospheric mantle to form isotopically enriched magmas (Dostal et al., 2003). Alternatively, asthenospheric flow may be largely lateral in direction, with the slab window serving as a vent for transfer from one mantle reservoir into another (Johnston and Thorkelson, 1997; Murdie and Russo, 1999). As with the forearc, the arc and back-arc regions may undergo crustal anatexis in response to mantle upwelling and mafic magmatism. The diachronous effects of a migrating slab window are outlined by Thorkelson (1996).

Slab anatexis can augment the mantle-related processes at work in slab window environments. The idea of thermal erosion of a slab window margin was introduced by Dickinson and Snyder (1979) who noted the difference between a geometrically defined slab edge and a thermally modified one, in the case of the Farallon–Pacific slab window presently situated beneath the southwestern US. This concept was extended by Severinghaus and Atwater (1990) who compared the amount of thermal energy used in the formation of oceanic lithosphere with the amount of thermal energy transferred to oceanic lithosphere during subduction. Their calculations showed that young subducted slab would be efficiently re-heated during subduction and become rheologically indistinguishable from the surrounding mantle. When they applied their formulation to the Farallon–Pacific slab window beneath the southwestern US, they found that the effective edge of the slab window margin would have been hundreds of kilometers from the geometrical edge defined by Dickinson and Snyder (1979), and that a "slab gap" within the subducted Farallon plate would have begun to form millions of years prior to ridge–trench intersection. However, specific igneous processes such as anatexis, melt extraction and restite behaviour were not addressed by Severinghaus and Atwater (1990), and the magmatic significance and physical extent of the "slab gap" remain uncertain. Nevertheless, their analysis underlined the importance of considering the effects of heating young oceanic crust during subduction. Studies in Chile (Kay et al., 1993), Central America (Johnston and Thorkelson, 1997), Baja California (Benoit et al., 2002), and western Canada (Breitsprecher et al., 2003) have identified adakitic melts in the proximity of Cenozoic slab windows. These findings complement the earlier study of Rogers and Saunders (1989) on magnesian andesites, and solidify the connection between ridge subduction and slab melting.

3. Partial melting of subducted oceanic lithosphere

The degree to which anatexis of subducted oceanic crust has contributed to magmatism in convergent plate margins has been a point of controversy for decades. As discussed by Gill (1981), arc magmas of basaltic composition are regarded as products of mantle, not slab, anatexis, although some later workers continued to press for slab anatexis in the production of arc basalts, particularly those with high Al-contents (e.g., Brophy and Marsh, 1986). Hydrated mantle peridotite as the principal source for arc basalts is now firmly established (e.g., Tatsumi, 1989; Arculus, 1994), but the genesis of intermediate and felsic arc magmas remains controversial. Most intermediate to felsic magmas in volcanic arcs are regarded as products of various processes spanning a continuum from fractional crystallization of arc basalt, to assimilation of crustal rock by arc basalt, to crustal anatexis and magma mixing (e.g., Gill, 1981). Nevertheless, some intermediate to felsic magmas, although subordinate in most Phanerozoic magmatic arcs, may be more favourably regarded as products of slab anatexis, as detailed below.

The issue of slab anatexis as a globally important process was emphasized by Defant and Drummond (1990) and Drummond and Defant (1990) who demonstrated a connection between subduction of young oceanic crust and production of intermediate to felsic igneous rocks which bear the signature of a garnetiferous residuum. Such magmatic rocks are compositionally similar to Tertiary lavas on Adak Island in the Aleutian arc which were identified as products of slab melting by Kay (1978). This petrologic family, termed *adakites*, was described by Defant and Drummond (1990) as high-alumina, intermediate to felsic volcanic rocks typically hosting phenocrysts of plagioclase, amphibole, mica and (rarely) orthopyroxene, and lacking phenocrysts of clinopyroxene. Accessory grains of titanomagnetite, apatite, zircon and titanite were identified as common but not ubiquitous. A complementary and broadly accepted chemical definition of adakites was subsequently provided by Defant and Kepezhinskas (2001): adakites are high-silica (SiO_2>56%), high-alumina (Al_2O_3>15%), plagioclase and amphibole-bearing lavas with Na_2O>3.5%, high Sr (>400 ppm), low Y (<18 ppm), high Sr/Y(>40), low Yb (<1.9), and high La/Yb>20.

The connection between subduction of youthful crust and genesis of adakites fueled both new research and new controversy (e.g., Green, 1994; Garrison and Davidson, 2003). Support in the petrological community for anatexis of young slab is now well established in many studies. Experimental work and case studies favour the production of some adakitic magmas by reaction of slab melts with peridotite in the mantle wedge as they rise toward the overriding crust (Kepezhinskas et al., 1997; Rapp et al., 1999). Arguably the most contentious issue is the nature of the geological environment where partial melting of slab is likely to occur.

The thermal structure of subduction zones as modeled by Peacock et al. (1994) and Peacock (1996) supports the general concept of melting of young oceanic crust. In detail, however, this model predicts melting in only very young crust (<5 Ma) whereas the data sets of Drummond and Defant (1990) and Maury et al. (1996), which summarize known adakite occurrences, suggest that anatexis occurs in slabs as old as 20 Ma. The difference between the predicted and actual distributions of adakites is largely a function of the shear stress values applied in the thermal modeling. Peacock (1996) preferred to model *P–T* conditions assuming shear stress heating is negligible, resulting in melt production only in very young slabs. Other workers, however, have favoured shear stress values as high as 66 MPa, resulting in higher model temperatures in the subducted crust, and thereby predicting melting in slabs as old as 40 Ma (Green and Harry, 1999). Understanding the occurrence of documented adakites where thermal models predict they should be absent (Bourdon et al., 2002) remains fundamental to a more complete understanding of convergent margin magmatism. Examination of slab window environments, where theoretical and empirical studies agree on the issue of slab anatexis, may provide a platform for future investigations into adakites, thermal structure, and subduction zone dynamics.

4. *P–T* paths and phase equilibria of slab window margins

Determining the metamorphic and anatectic path for a specific subduction zone requires specific knowledge of a large number of factors. The most important of these include *P–T* conditions, progression of dehydration, metamorphic and partial melting reactions, subduction geometry, convergence rate, and plate velocity. Each of these factors is, in turn, governed by parameters which may vary within a broad range. In the case of *P–T* conditions, some of these parameters include plate age, degree of shear stress, and the temperature of brittle-plastic transition in rheology (Peacock et al., 1994). Regarding dehydration, parameters include the initial concentration of water in the slab and its form of transport (e.g., pore space; hydrous rock-forming minerals). Many of the factors are interrelated and may be regarded as feedback loops, an example of which is a probable decrease in viscous coupling and shear heating between slab and overlying mantle brought about by release of water or silicate melts along the slab–mantle interface. Several workers have attempted to quantify the main factors of subduction and have provided numerical solutions and graphical displays to describe a variety of subduction zone types (e.g., Peacock et al., 1994; Harry and Green, 1999). Iwamori (2000) provided a two-dimensional thermal model of ridge subduction, but the model ridge did not diverge to form a slab window and Iwamori was therefore unable to address the fate of slab edges bordering a slab window.

To investigate anatexis of slab feather edges bounding a slab window, we selected a set of *P–T* curves calculated for subduction of young oceanic crust (0–20 Ma) with the value of shear stress set to zero (Peacock, 1996). We then estimated the positions of *P–T* curves for a moderate value of shear stress (33 MPa), according to differences between a set of two curves calculated for a slab age of 50 Ma, with shear stress values of 0 and 33 GPa, respectively (Peacock, 1996). We have adopted a shear stress value of 33 MPa because it lies mid-way between the differing values of shear stress (0 to 66 MPa) applied in existing subduction models. The value is supported by recent attempts to quantify frictional heating from empirical heat-flow studies undertaken at modern subduction zones. van Keken et al. (2002) found the Honshu subduction system to have shear stress values of approximately 10 MPa; Ruff and Tichelaar (1996) found that average shear stress from modern subduction zones ranges from 14 to 30 MPa, depending on whether the frictional heating is linear or incremental throughout the seismogenic zone. Further support for a moderate shear stress value comes from the spatial relationship between Cenozoic adakites and slabs with ages exceeding 20 Ma, a correlation which seems to require significant shear heating, i.e., high values of shear stress. As noted by Green and Harry (1999), melting in slabs as old as 40 Ma would be expected where values of shear stress exceed 60 MPa.

The interpolated set of *P–T* curves, which represent approximate conditions at the top of the downgoing slab for a convergence rate of 100 km/Ma, a slab dip of 30°, and moderate shear stress value of 33 MPa, are shown in Fig. 2 along with information on mineral stabilities and partial melting of hydrated basalt (and its metamorphic equivalents). The curves are similar to those calculated for shallower depths (to 2 GPa) by Harry and Green (1999) who used a shear stress of 33 MPa for slabs of age 1, 5 and 10 Ma. Each curve represents the changing *P–T* conditions of a point on a subducting slab and is labeled according to the age it had when it began to subduct, herein termed slab *maturity*.

All of the *P–T* paths in Fig. 2, except the one for the 50 Ma slab, intersect the hydrous basalt solidus of Green (1982). The *P–T* path for subducting oceanic crust with a maturity of 20 Ma reaches the solidus at a depth of approximately 145 km. However, the slope of this path at that depth is sub-parallel to the solidus, so the point of intersection is not well constrained. Less mature slabs follow paths which intersect the solidus at higher angles in *P–T* space (at shallower depths), providing greater certainty in the estimated depths of melting. These paths show that a subducting slab with a 10-Ma maturity will begin to melt at approximately 105 km. For maturities of 5, 2 and 1 Ma, melting will

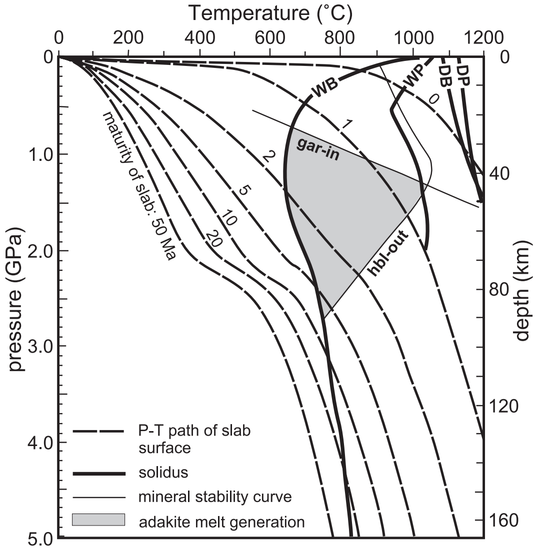

Fig. 2. Pressure–temperature and phase-stability diagram for subducting slabs of various ages. Slab *P–T* paths (dashed) modified from Peacock et al. (1994) to reflect moderate (33 MPa) levels of shear-stress. Labels on *P–T* curves indicate slab maturity, i.e., the age of slab when it entered the trench. Peridotite and basalt melting curves (wet and dry) from Harry and Green (1999); hornblende-out line from Peacock et al. (1994); garnet-in line from Cloos (1993). Shaded field indicates conditions favourable for adakite magma genesis. Abbreviations used: DB=dry basalt, DP=dry peridotite, WB=wet basalt, WP=wet peridotite.

begin at approximately 80, 45 and 15 km, respectively. Maturities of 0 Ma, which represent the slab edge (a subducted ridge crest), will begin to melt at approximately 5 km. These depths of incipient anatexis apply only to the oceanic crust which is generally basaltic in composition; solidus curves for crust with other compositions (e.g., subducted sediment) were not evaluated. Furthermore, in all cases, the temperature at which melting begins, and the precise composition of the melt, are contingent on the degree of hydration. For poorly hydrated basaltic crust, melting will begin at temperatures somewhat higher than the water-saturated solidus of Green (1982), shown in Fig. 2. The underlying component of the slab, namely the subducted oceanic lithospheric mantle, is likely to be harzburgite (refractory peridotite) which will become more ductile with depth but may never melt except where it has been serpentinized, e.g., along transform faults or where ocean-floor hydrothermal alteration has been particularly extensive.

5. Adakitic and non-adakitic melt generation

The range of subduction paths shown in Fig. 2 indicates that slab anatexis is possible at depths from approximately 5–150 km. Within this broad range of slab melting there is a smaller field, where both garnet and hornblende are stable in the slab, in which magmas with adakitic melts can be generated. To achieve adakite compositions, amphibole is required as a reactant, and garnet is required as a stable residuum phase (Drummond et al. 1996). In *P–T* space (Fig. 2), the region of possible adakite formation lies in a field bordered by the “wet basalt” solidus, the garnet-in line and the amphibole-out line. *P–T* paths which pass through this field indicate that adakite melt generation is constrained to approximately 25–90 km. According to the subduction paths shown in Fig. 2, oceanic crust with maturities ranging from 5 Ma to slightly below 1 Ma will pass through this field and yield adakitic melts. Melts generated from slabs with less maturity (<0.5 Ma) and more maturity (5–20 Ma) will not bear the chemical signature of an adakite because one or more requisite phases are not stable. Adakitic magmas derived from slab anatexis are thought to have equilibrated with restite rich in garnet and pyroxene, with garnet responsible for low abundances of heavy rare earth elements (REE) in the melts. (Peacock et al., 1994; Drummond et al., 1996). The melts generated at shallow depths (<25 km) correspond to slab maturities <1 Ma and are likely to be broadly granodioritic to tonalitic in composition (Wyllie, 1984; Beard et al., 1991; Peacock et al., 1994; Lopez and Castro, 2001) rather than adakitic, because of the lack of garnet in the restite. These non-adakitic melts are expected to have relatively flat REE profiles on mantle- or chondrite-normalized diagrams and, more specifically, non-adakitic Yb abundances (>1.9 ppm), La/Yb ratios (<20) and Sr/Y ratios (<40). Melts generated at depths >90 km, corresponding to slab maturities from 5–20 Ma, are likely to show steep REE profiles characteristic of garnetiferous residuum (i.e., similar to those of adakites), but few such melts may form because slab conditions at that depth may be relatively anhydrous.

These general observations, however, need to be further qualified in the case of a slab window margin because of the pronounced increase in slab temperature toward the window. As the temperature changes, phase stabilities are no longer simple depth-dependent features, and are therefore not simply related to distance from the trench. Each phase must be mapped out, in terms of both the pressure and temperature of the slab. The result is a series of phase boundaries which are approximately trench-parallel at distances far from the slab window, but which deflect to either deeper or shallower depths as the subducted lithosphere becomes hotter toward the slab window. The model positions of these curves are all contingent on the specific thermal model and degree of slab hydration chosen, as discussed by Peacock et al. (1994).

6. Physical and temporal parameters of slab window margins

In preparation for an integrated physical and chemical model of slab anatexis, we have drawn an idealized slab window (Fig. 3). The slab window is highly simplified in that it has no transform offsets, the ridge is perpendicular to the trench, and the ridge–trench–trench triple junction is stationary. The slabs dip at 30°, the subduction rate is 100 km/Ma, and the oceanic divergence half-rate (material accreted per plate) is 30 km/Ma, as shown graphically by the 1 Ma-increment plate vectors on the diagram, drawn relative to the overriding plate (not shown). In simplest terms, the resulting environment is a pair of slabs which thin

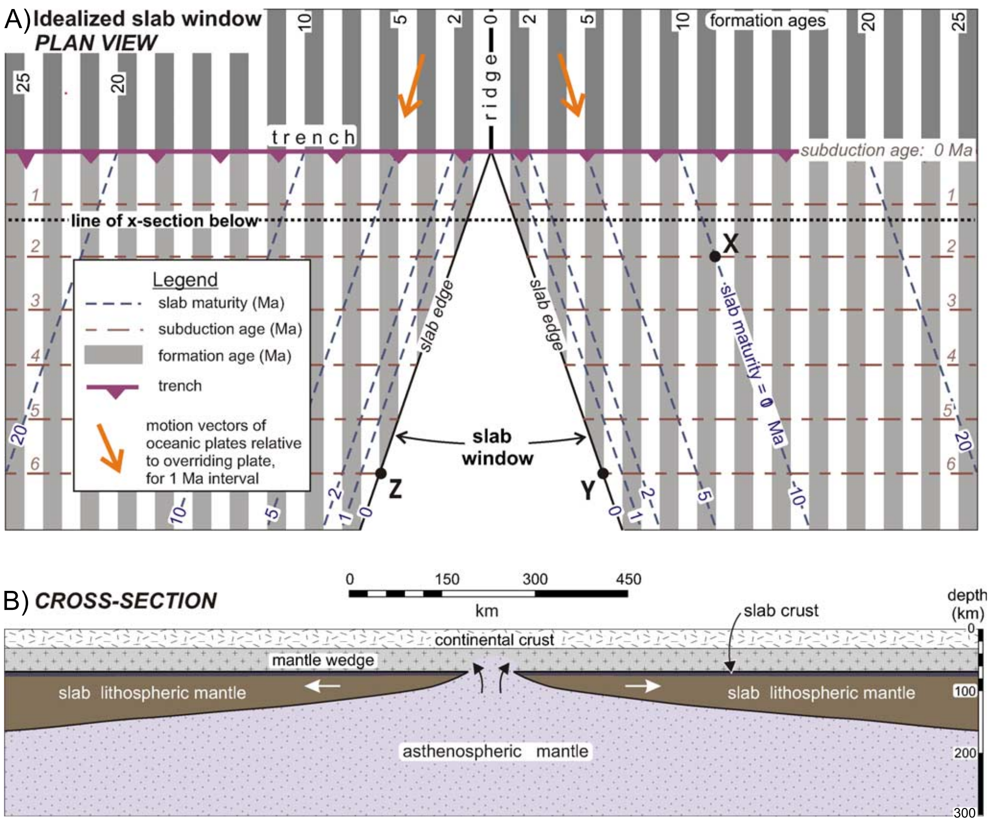

Fig. 3. Relations among formation-age, subduction-age and lithospheric thickness of slabs in a slab window environment. (A) Plan view of symmetrical slab window, with overriding plate transparent to show features on the subducted slabs (faded region). Parameters used in construction: convergence rate between subducting plates and overriding plate=100 km/Ma; full-spreading rate between subducting plates=60 km/Ma; slab dip=30°. (B) Cross-section showing relations among the slabs, asthenospheric mantle, mantle wedge and continental crust. Depth to top of slab is 65 km. Arrows in asthenosphere show possible upwelling. Thermal model used to calculate tapered geometry of oceanic lithosphere is GDH1 (Stein and Stein, 1996). Thermal erosion of slabs is not illustrated; compare with Fig. 5.

progressively toward the slab window, reaching a zero-thickness edge at the window margin. The window itself is a slab-free region which may serve as a pathway for flow of peridotite between sub-slab and supra-slab mantle reservoirs (Thorkelson, 1996).

We have gridded the slabs by lines of equal *formation-age*, *subduction-age*, and *slab maturity*. Understanding the definition and significance of these iso-lines is essential prior to analyzing the spatial distribution of mineral stabilities and regions of anatexis. The *formation-age* of a specific part of a subducting slab is the time when it formed at the ridge crest. The *subduction-age* of a given point on the slab is the time elapsed since it entered the trench and began to subduct. The *slab maturity* of a specific point is defined as the formation-age it had when it began to subduct. More mature parts of the slab spent longer intervals as sea-floor, becoming thicker and cooler as they diverged from the spreading axis, prior to subduction. Lines of constant formation-age are essentially continuous with sea-floor stripes on the unsubducted ocean floor, and their spacing is a function of spreading rate (30 km/Ma in the case shown in Fig. 3). Lines of constant subduction-age run parallel to the trench and their spacing reflects the rate of subduction. Lines of constant maturity run parallel to the slab window margin and their spacing is constrained by the relative rates of spreading and subduction. In Fig. 3, point X has a formation-age of 12 Ma, a subduction-age of 2 Ma, and a maturity of 10 Ma.

The feather edges of the slabs in Fig. 3 (the slab window margins) represent subduction of a long, continuous ridge crest. The edges therefore have a maturity of 0 Ma but range in formation-age from 0 Ma at the current ridge–trench–trench triple junction to several Ma at depth. The lines of constant formation-age intersect the slab window margin. At a given point of intersection, the formation-age of the slab indicates when that point was at the ridge–trench–trench triple junction, i.e., when that part of the former ridge crest was beginning to subduct. For example, the part of the ridge crest which entered the trench at 6 Ma is located at the intersection between the window margin and the 6 Ma-line of constant formation-age (point Y on Fig. 3). This part of the slab formed 6 million years ago, but spent its entire life in a subduction environment, and therefore has a maturity of 0 Ma. This statement applies to both of the slabs bounding the slab window, so that the equivalent 6 Ma intersection-point on the opposing slab (point Z in Fig. 3) was, at 6 Ma, adjacent to point Y on the mid-ocean ridge as that part of the ridge was starting to subduct. In the general case where relative plate velocities are not equal, these points on each plate, and the associated subduction-age iso-lines, would not be equidistant from the trench. The rate of subduction (100 km/Ma in Fig. 3A) is such that these points on the window margins, and all parts on each of the slabs which are an equal distance from the trench, have subduction-ages of 6 Ma.

Slab thickness is a function of both slab maturity and subduction-age. As oceanic crust moves away from a ridge crest and cools, its underlying lithospheric mantle progressively thickens (Crough, 1975; Stein and Stein, 1996). Thickness achieved from progressive cooling of ocean floor reaches a maximum where the plate encounters a subduction zone. As the lithosphere begins to subduct, the process of cooling and thickening is arrested and, as it plunges into the hot asthenosphere, it begins to heat and thin. The lithospheric thinning occurs by two general processes, both of which are covered by the term *thermal erosion* (Thorkelson, 1996; Sleep et al., 2002). In the first process, which applies to all cases, the deepest and thinnest portions of the slab's mantle lithosphere thermally erode as they rise in temperature, lose rigidity, and become rheologically indistinct from the subjacent asthenosphere (e.g., Severinghaus and Atwater, 1990). In the second process, which applies mainly to lithosphere of low maturity, the crustal component of the subducting slab thins through partial fusion and uprise of anatectic melts. A cross-section through the slab at constant subduction-age (parallel to the trench) shows how slab thickness would vary with distance from the slab feather edge, in the absence of thermal erosion (Fig. 3B). This idealized or "geometrical" profile is a convenient framework for the subsequent analysis of slab anatexis.

7. Dynamic modeling and melt zonation

7.1. Petrologic zonation

To understand the physical distribution of slab anatexis, we have applied information from *P–T* studies and thermal modeling (Fig. 2) to the tectonic framework laid out in Fig. 3. This approach demonstrates that the edges of slabs bounding a slab window are likely to undergo extensive melting, and that a complex petrologic zonation exists within the region of melt generation. Our first step in this analysis was to transfer the hydrous basalt solidus from *P–T* space to the slab window diagram. This was done by first noting the pressure coordinate for each intersection between the solidus and the subducting slab paths (Fig. 2). Each of the slab paths in Fig. 2 is equivalent to a line of maturity on the slab (Fig. 3), and each pressure value is equivalent to a slab depth. Using these equivalencies, we located the position (depth) of the solidus for several lines of maturity, and interpolated among the points to draw the solidus curve directly on the slab surface (Fig. 4A). This procedure was then followed for the hornblende-out and garnet-in mineral stability curves, both of which are critical to the prediction of magmas with adakitic compositions.

The location of the wet basalt solidus in Fig. 4A indicates that the subducted igneous oceanic crust will undergo anatexis in the vicinity of the window margin (assuming sufficient hydration). As predicted from the *P–T* diagram in Fig. 2, this melt zone begins near the trench at a depth of about 5 km; in addition, it can now be seen that the melt zone progressively widens with depth. Hornblende is stable in part of the melt zone from near the trench to a depth of nearly 90 km. Garnet is stable below depths ranging from 25 to 50 km. In this depth-range, the width of the melt zone (in the plate environment specified in Fig. 3) is about 55 km wide and affects slab with a maturity of <2 Ma. According to Thompson and Ellis (1994).), genesis of adakitic magma occurs where both hornblende and garnet are stable, i.e., between the hornblende-out and garnet-in stability curves (Fig. 4A). The exact positions on the slab of all of these curves depend on the physical and thermal parameters used to construct the model.

How can we use these mineral and melt curves to understand anatexis of the slab window margin? The simplest way is to assume that the curves represent steady-state conditions in *P–T* space, but that the slab moves through these conditions as it subducts. As a given part of the slab descends, it moves across various mineral stability curves along vectors parallel

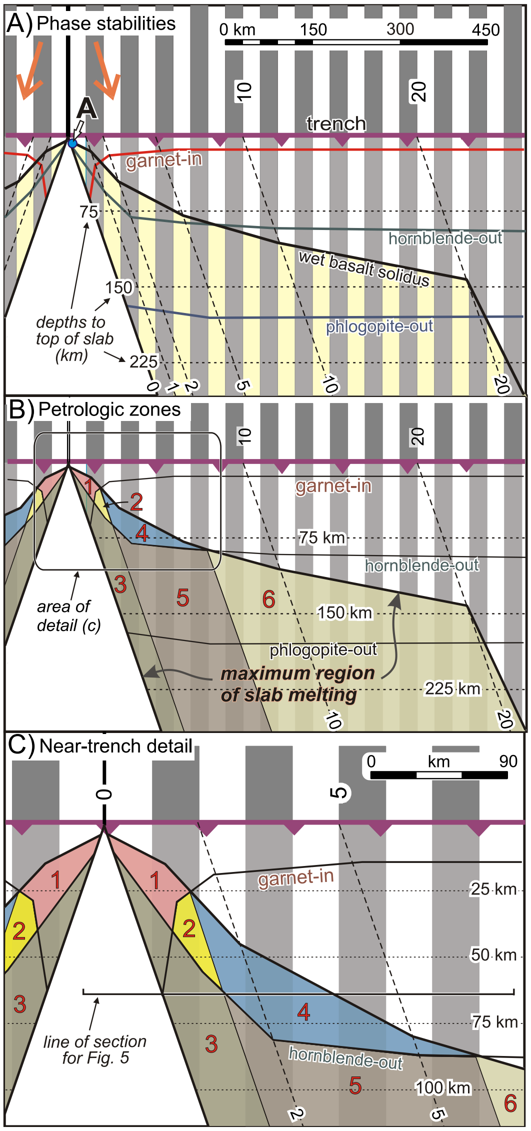

Fig. 4. Melt and phase stability for slab *P–T* conditions in a slab window environment. Slab window kinematics as in Fig. 3. (A) Phase stabilities and wet basalt solidus, transferred from Fig. 2. Dashed lines represent slab maturity; dotted lines represent depth to the top of the slab. (B) Petrologic zonation of slab resulting from passage of slab through steady-state regions of metamorphism and anatexis. (C) Detail of inset map shown in B. Zone 1: non-adakitic melting. Zone 2: restite zone from (1) plus minor adakitic melt generation. Zone 3: restite from Zones 1 and 2, plus possible melt generation of garnet-signature melts. Zone 4: adakite melt generation (never before melted). Zone 5: restite from adakite melt generation and possible continued melting (garnet restite). Zone 6: possible anatexis of eclogitic slab (never before melted). Section line relates to Fig. 5.

to the slab edges, and undergoes a sequence of thermal and chemical changes in a series of progressively higher metamorphic facies. Changes to the slabs, including mineral reactions, fluid release and partial fusion, thereby occur sequentially as they descend to greater depths. Using this dynamic approach, we recognize six distinct petrologic zones (Fig. 4B) in which the slab has been affected by melting, based solely on the stability curves for amphibole and garnet. Each of the zones is defined by changes inherited from shallower zones in combination with changes imparted by the ambient *P–T* conditions within each zone. This zonation provides basic constraints on the locations of melting, and sheds light on the distribution of adakitic vs. non-adakitic slab-derived magmas in slab window environments. More complex zonation could be defined by considering a greater number of stability curves, but that analysis would result in a plethora of zones, and will not be carried out here.

7.2. Zone 1

In the model shown in Fig. 4B, partial melting first occurs at a point along the feather edge at the surface of the slab, at approximately 5-km depth (point A). As the plate continues to descend, the melting front migrates in two directions: (1) away from the slab edge and into subducted crust of greater maturity, and (2) away from the upper surface of the slab and into lower layers of the subducted crust, i.e., toward the underlying lithospheric mantle (cf. Harry and Green, 1999). The portion of the slab which is undergoing melting (zone 1) is progressively converted to migmatite. The anatectic melts form channels among solid phases in the migmatite, and rise upward due to buoyancy. The melts are broadly granodioritic to tonalitic in composition (Wyllie, 1984; Beard et al., 1991; Lopez and Castro, 2001) and leave behind a restite of garnet-free amphibolite to pyroxenite. Melting is most extensive along the feather edge which becomes largely converted to restite. Synchronously, the oceanic lithospheric mantle of the slab becomes progressively hotter and more ductile, particularly at the feather edge.

The feather edge (maturity<0.5 Ma) does lie within the field of dry basalt melting (Fig. 2), so that in the absence of hydration, it may begin to melt at depths of 30–50 km. However, if hydrous minerals exist in the feather edge, it will first undergo hydrous melting. If the melts then separate from the restite (as expected), subsequent (anydrous) fusion of the refractory residue may not occur.

7.3. Zones 2–3

As the slab descends further, the part of the slab which underwent melting in zone 1 moves across the garnet-in isograd at depths between 25 and 50 km. As this stability curve is crossed, melting continues and garnet begins to grow in the residuum (zones 2 and 3). Amphibole is stable in zone 2 but not zone 3, and the significance of this division is that adakitic melts are more likely to be produced in zone 2, where amphibole is available as a reactant in melting (Thompson and Ellis, 1994; Drummond et al., 1996). However, both zones 2 and 3 are similar in that (1) they are likely to have garnet as a residual phase, and (2) the crust in those zones was previously subjected to melting in zone 1. Because of the earlier melt extraction, the crust entering zones 2 and 3 has depleted abundances of water and incompatible elements, and reduced fertility for melting. In particular, zone 3 is essentially anhydrous and may yield little additional magma, particularly along the feather edge which had been largely “melted out” and converted to a refractory residuum.

7.4. Zones 4–5

Zone 4 is the “adakite zone” where most adakites are likely to be generated. Subducted crust entering zone 4 has undergone prograde metamorphic reactions but not anatexis. Both amphibole and garnet are stable in zone 4, and partial fusion of the slab results in a migmatite consisting of adakitic magma and a largely eclogitic restite (Peacock et al., 1994; Drummond et al., 1996). Melts rising from this zone carry away many of the fertile components. As the subducting crust passes from zone 4 into zone 5, amphibole is eliminated and further melting (in zone 5) is likely to be small in volume. In this sense, the petrologic properties of zone 5 are similar to those of zone 3. If melting were to occur in zone 5, it would bear the signature of a garnetiferous residuum, possibly garnet websterite.

7.5. Zone 6

Zone 6 is similar to zone 4 in that it receives metamorphosed but unmelted slab from higher in the system. The metamorphism includes dehydration reactions for amphibole so that by the time slab crosses the wet basalt solidus and moves into zone 6, it has been largely altered to eclogite. This conversion to a mainly anhydrous rock retards anatexis, and the "wet basalt" melting curve may not, therefore, represent the onset of melting in zone 6; much of zone 6 may actually be melt-free. However, small amounts of phlogopite or other hydrous minerals may continue to be stable at depths up to 200 km and their breakdown may establish locally hydrous conditions and help to induce slab melting. Any magmas produced in zone 6 are likely to be low-percentage melts with steep REE profiles, and should leave behind a garnet-bearing residuum.

7.6. Cross-sectional view

A detailed model of slab anatexis is presented in Fig. 5 as a cross-section through a slab edge at a depth of 65 km. The section line, shown in Fig. 4C, transects three main petrologic regions. Farthest away from the slab's feathered tip, the subducted crust has been metamorphosed and probably consists largely of garnet-bearing amphibolite (Peacock et al., 1994). Closer to the tip, in zone 4, the subducted crust is actively melting. Adakitic magma is rising and leaving behind an eclogitic restite. The tip of the subducted crust (zone 3) consists of eclogitic restite from which small volumes of melt may be forming. Previously, when this region was passing through zones 1 and 2, it underwent extensive melting, yielding non-adakitic and possibly some adakitic melts.

The subducted mantle lithosphere shown in Fig. 5 has also undergone changes. Originally, it probably consisted of harzburgite generated at a mid-ocean ridge. During subduction, this depleted peridotite became subjected to progressively higher temperature conditions, and is currently in the garnet stability field (although aluminous phases such as garnet may be scarce or absent). As the temperature of the slab increased, so did its ductility. The base and tip of the slab mantle are likely to have become so hot that it is now rheologically indistinguishable from the surrounding asthenosphere (Severinghaus and Atwater, 1990), permitting those portions of the slab to flow ductily with the asthenosphere as it convects.

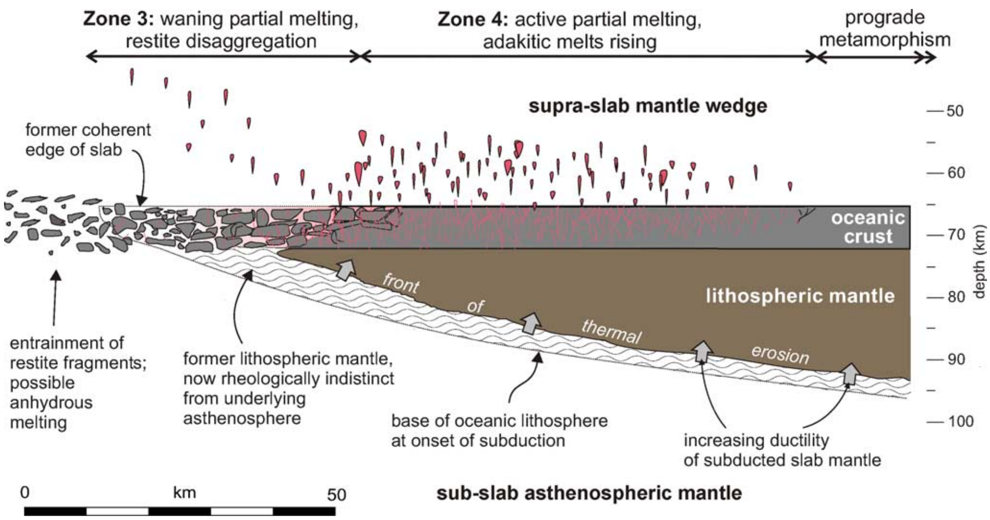

Fig. 5. Thermal erosion of a slab window margin shown as a vertical cross-section through the slab in Fig. 4C. Section cuts through anatectic zones 3 and 4 (described in text). Zone 3 consists mainly of disaggregated restite generated from melting in zones 1 and 2. Note possible entrainment of restite in ambient mantle. Zone 4 is region of adakite magmagenesis. To the right of zone 4, the crust has been metamorphosed to largely eclogite. Underlying lithospheric mantle becomes progressively more ductile and rheologically similar to the asthenosphere.

8. Oblique ridge subduction

To this point, our modeling has been displayed on a non-migrating, symmetrical slab window. This configuration is an end-member in the range of geometrical possibilities for ridge–trench intersections and their resultant slab windows (Thorkelson, 1996). To achieve more realism, we present a more general case in which the ridge and trench intersect at a moderate angle, the triple junction and slab window migrate, and zonation of melt zones is asymmetrical (Fig. 6). This scenario is still simplified over real-word examples in that the spreading ridge is not offset by oceanic transform faults. Nevertheless, it is able to show the important principle that opposing slab edges generally have very different patterns of melt zonation.

In Fig. 6A, plate A is subducting obliquely at 35 km/Ma, whereas plate B is subducting near-orthogonally at 62 km/Ma. The asymmetry of the plate motions in the example presented results in a ridge–trench–trench triple junction that migrates southward at a rate of 46 km/Ma. The slab window opens to the northeast and its margins are undergoing melting. The pattern of melt zonation, however, is very different. Melting on plate A is confined to its feather edge whereas melting on plate B is more extensive. Both slabs are yielding adakitic and non-adakitic magmas. However, if plate A were subducting even more obliquely, its feather edge may not reach depths in the garnet stability field for great distances from the triple junction, and by that point extraction of non-adakitic melts may have rendered the melt zone infertile.

A main consequence of the southward migration of the slab window is that the magmas generated by slab anatexis are released progressively farther south as subduction proceeds. This southward trajectory of melt-release is part of a broader regime of melting involving hydration-melting of the mantle above the slabs (normal arc magmatism) and decompressional melting of uprising mantle within the slab window (Fig. 6B). The overlying mantle and crust will therefore be affected by streaks of slab-melts rising within a dynamic igneous and metamorphic system. Some portions of these streaks may reach the surface with little contamination, but much of the slab-melt flux is likely to interact with mafic magmas, mantle peridotite, or crust of the overriding plate to yield hybrid or contaminated magmas (cf. Drummond et al., 1996).

9. Orphaned slab restite

As the effective slab edge retreats through thermal erosion, slab restite may be progressively abandoned by the slab and transferred to the ambient mantle. This

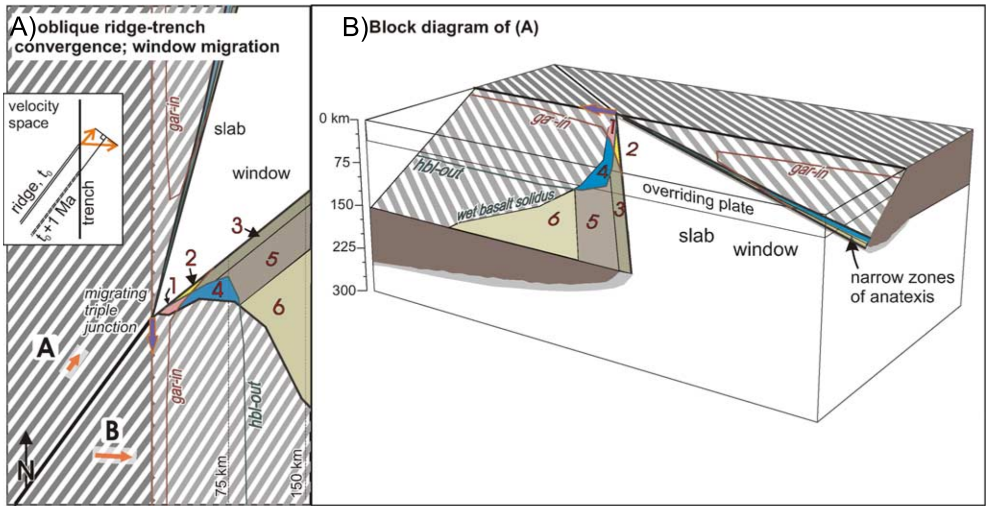

Fig. 6. Asymmetrical geometry of melting zones for a slab window resulting from oblique convergence of a spreading ridge with a trench. Motion vectors of plates A and B shown by heavy arrows. Triple junction and slab window migrate southward. (A) Plan view, slab dips=30°. Velocity diagram shown as inset. (B) 3D block view of the window shown in A.

intriguing possibility may be envisaged by the following scenario in which solid slab converts to migmatite, loses cohesion and separates from the subducting lithosphere. The net result of thermal erosion of both slab crust (by anatexis and removal of restite) and slab mantle (by increasing ductility) is a thinner, shorter mechanical slab and a wider slab window.

As the subducted crust melts, a front of migmatization moves both laterally from the slab tip to regions of greater maturity, and downward from top of the slab crust to the underlying slab mantle. Deeper parts of the slab crust may be less hydrated and may resist melting. The migmatite is likely to consist of restite fragments (largely eclogite) that are crosscut and enclosed by flowing adakitic to tonalitic melt. The restite fragments may range in size from boulder-size blocks to individual mineral grains. The melt percolates along grain boundaries, collects in feeder channels, and rises in dykes, disintegrating the slab crust at a variety of scales. The migmatite has little strength, and its physical connection to lower layers in the slab is progressively diminished as melting advances. As the subducting slab shears through the mantle, some—perhaps most—of the migmatite detaches from the slab and becomes incorporated into the mantle. As the front of migmatization migrates deeper into the slab, the earlier-formed restite becomes progressively stripped away, contaminating the surrounding mantle and exposing lower levels of the slab.

Depending on factors such as mantle structure and depth of anatexis, the restite contaminants may become part of either the lithospheric or asthenospheric mantle reservoirs. Where they become lodged in the lithosphere, they become transferred to the overriding plate. In the case of a continental margin environment, restite fragments lodged in the overriding plate may become long-term constituents of the continental lithospheric mantle. Conversely, where the restite fragments become entrained in the asthenosphere, they may flow along with the convecting peridotite in a pathway distinct from the trajectory of the slab itself, and travel far from the locus of subduction. The restite fragments will behave ductily within the flowing asthenosphere, becoming pyroxene- and garnet-rich streaks.

Shear-removal of disaggregated slab restite from the surface of a slab is a plausible way of providing compositional variety to both the continental tectosphere and the underlying convecting mantle. This process appears to be particularly likely for slab window environments, where slab antexis is most feasible. We suggest that orphaned slab restite may be a principal contributor to both "plum pudding" mantle (Carlson, 1988) and anomalous compositions of igneous rocks erupted in oceanic and continental settings. If, for example, Nb is preferentially stabilized and retained in restite (e.g., Saunders et al., 1988), then zones of restite-rich mantle generated in slab window margins may, under subsequent conditions of upwelling, hydration or heating, become sources for Nb-enriched basalt. Therefore, the overall effect of slab melting on the distribution of Nb may be twofold: to yield Nb-depleted adakitic and non-adakitic magmas which rise into the overlying lithosphere; and to leave behind Nb-enriched restite which may, in turn, become heterogeneities in the upper mantle.

10. Importance of mantle flow

The theoretical approach taken in this paper provides a general model for understanding the chemical geodynamics of slab window margins. This model, however, provides a description of only part of the overall tectonic and geochemical system of slab windows. Some additional comments on variables in the model, and other processes at work, may provide a more complete understanding.

The flow pattern of mantle in and near slab windows is of particular interest. In most tectonic models of subduction zones, mantle motion is considered be passive corner-flow induced by viscous coupling of mantle to descending slab (e.g., Saunders et al., 1991). This style of mantle flow forms the basis for the thermal models of Peacock (1993, 1996) and Peacock et al. (1994), which we have applied in this paper. However, the actual flow path of mantle in and near a slab window may be quite different. A principal reason for the difference is that the subducting ridge is coupled to a passive cell of upwelling asthenosphere. This upwelling is caused by plate divergence, which continues after the ridge subducts even though a gap separates the subducted slabs at depth. The cell of upwelling, therefore, may become increasingly diffuse with depth, but is nevertheless a factor in determining the overall flow path (Thorkelson, 1996). In addition, the slab window may serve as a pathway for lateral mantle flow, as in the case of Central America (Johnston and Thorkelson, 1997).

The importance of recognizing the complexity of mantle flow is twofold. First, mantle flow paths will have an effect on the temperature of the slab edges. In particular, upwelling will bring hotter mantle in contact with the slabs, increasing their rate of thermal erosion. Second, the direction of mantle flow will govern the paths taken by anatectic melts and streaks of restite. Anatectic melts will tend to rise because of their relative buoyancy, but their actual trajectory may be affected by mantle flow, causing them to enter the lithosphere in a position which is offset from their source. Restite streaks, in some cases, may flow along with the slabs, thereby following them deeper into mantle. In other situations, restite streaks may be entrained by convecting mantle and flow upwards or laterally. Upward flow may cause them to melt by decompression. Lateral flow paths may shift the streaks to a variety of locations including those beneath the arc, back-arc, or mid-ocean ridge. A band of restite streaks carried to deep or distant locations is an attractive way to generate long-term mantle heterogeneities.

11. Synthesis

In slab window environments, feather edges of slabs separate from one another and undergo melting. The locations of anatexis, and compositions of melts and restites, are largely controlled by the stability curves for amphibole and garnet. Anatexis is likely to be prevalent where amphibole is available as a reactant in melt-generation. Where amphibole is involved, both adakitic and non-adakitic melts may be generated. Non-adakitic granodioritic to tonalitic magma forms along the feather edge at pressures below that of garnet stability. Adakitic magma is generated where garnet is stable as a restite phase, at some distance away from the slab edge. Still farther away, in crust of greater maturity and lower temperature, the slab undergoes metamorphism and dewatering but not melting. As the slab descends, regions of different maturity pass through different sequences of metamorphism and magmatism, producing a petrological zonation of the slab in the region adjacent to its edge. Concurrently, the underlying lithospheric mantle of the slab will progressively rise in temperature and ductility, and may begin to flow along with the ambient asthenosphere.

The exact location of the petrologic zones depends on a variety of factors, including degree of slab hydration, rate of plate divergence, rate and angle of subduction, amount of shear strain, and style of asthenospheric flow. We have limited our analysis to simple models but our results should be broadly applicable to many slab window configurations. However, in very asymmetrical slab windows formed from highly oblique ridge subduction, only one of the slabs may subduct to depths necessary to generate magma. The other plate, if it does subduct, may descend gradually, dehydrate slowly at shallow depths and become less prone to melting, or not melt at all. In the Archean, the slabs may have been hotter and the zones of melting more extensive; melting of slab window margins may have been important in the genesis of voluminous granitoid plutons.

Migration of a slab window results in a time-transgressive release of slab melts into the overlying mantle. Concurrently, slab-restite may separate from the slab surface and feather edge, and become incorporated into the ambient mantle. The release of both melt and restite represents a significant return of basaltic material to the mantle, albeit in two distinct phases. Re-introduction of components from the oceanic crust to the mantle in slab window environments may, therefore, be a principal outcome of ridge subduction. Reaction of slab melts with mantle peridotite is a significant aspect of this replenishment. Lodging of restite fragments within the continental lithospheric mantle, and the introduction of restite streaks to the asthenosphere, may also replenish the mantle in certain components and yield long-term mantle heterogeneities.

Acknowledgements

Funding was provided by NSERC and the Slab Window project of the US Geological Survey, Alaska. Stephen Johnston is thanked for the previous discussions on mantle replenishment. Julianne Madsen and Ryan Ickert are thanked for their input on slab window tectonics and anatexis. Reviews by Robert Ayuso and an anonymous referee led to significant improvements.

References

Arculus, R.J., 1994. Aspects of magma genesis in arcs. Lithos 33, 189–208.

Beard, J.S., Lofgren, G.E., 1991. Dehydration melting and water-saturated melting of basaltic and andesitic greenstones and amphibolites at 1, 3, and 6.9 kb. Journal of Petrology 32 (Part 2), 365–401.

Benoit, M., Aguillón-Robles, A., Calmus, T., Maury, R.C., Bellon, H., Cotton, J., Bourgois, J., Michaud, F., 2002. Geochemical diversity of late Miocene volcanism in southern Baja California, Mexico; implication of mantle and crustal sources during the opening of an asthenospheric window. Journal of Geology 110, 627–648.

Benz, H.M., Zandt, G., Oppenheimer, D.H., 1992. Lithospheric structure of northern California from teleseismic images of the upper mantle. Journal of Geophysical Research 97, 4791–4807.

Bourdon, E., Eissen, J.P., Monzier, M., Robin, C., Martin, H., Cotten, J., Hall, M.L., 2002. Adakite-like lavas from Antisana volcano (Ecuador); evidence from slab melt metasomatism beneath the Andean northern volcanic zone. Journal of Petrology 43, 199–217.

Breitsprecher, K., Thorkelson, D.J., Groome, W.G., Dostal, J., 2003. Geochemical confirmation of the Kula-Farallon slab window beneath the Pacific Northwest in Eocene time. Geology 31, 351–354.

Brophy, J.G., Marsh, B.D., 1986. On the origin of high alumina arc basalt and the mechanics of melt extraction. Journal of Petrology 27, 763–789.

Carlson, R.W., 1988. Mantle structure; layer cake or plum pudding? Nature 334, 380–381.

Cloos, M., 1993. Lithospheric buoyancy and collisional orogenesis; subduction of oceanic plateaus, continental margins, island arcs, spreading ridges, and seamounts. Geological Society of America Bulletin 105, 715–737.

Cole, R.B., Basu, A.R., 1995. Nd–Sr isotope geochemistry and tectonics of ridge subduction and middle Cenozoic volcanism in western California. Geological Society of America Bulletin 107, 167–179.

Crough, S.T., 1975. Thermal model of oceanic lithosphere. Nature 256, 388–390.

Defant, M.J., Drummond, M.S., 1990. Derivation of some modern arc magmas by melting of young subducted lithosphere. Nature 347, 662–665.

Defant, M.J., Kepezhinskas, P., 2001. Evidence suggests slab melting in arc magmas. EOS Transactions 82, 65–69.

Delong, S.E., Schwarz, W.M., Anderson, R.N., 1979. Thermal effects of ridge subduction. Earth and Planetary Science Letters 44, 239–246.

Dickinson, W.R., 1997. Tectonic implications of Cenozoic volcanism in coastal California. Geological Society of America Bulletin 109, 936–954.

Dickinson, W.R., Snyder, W.S., 1979. Geometry of subducted slabs related to San Andreas transform. Journal of Geology 87, 609–927.

D'Orazio, M., Agostini, S., Innocenti, F., Haller, M.J., Manetti, P., Mazzarini, F., 2001. Slab window-related magmatism from southernmost south America; the late Miocene mafic volcanics from the Estancia Glencross area (approximately 52 degrees S. Argentina–Chile). Lithos 57, 67–89.

Dostal, J., Breitsprecher, K., Church, B.N., Thorkelson, D.J., Hamilton, T.S., 2003. Eocene melting of Precambrian lithospheric mantle: analcime-bearing volcanic rocks from the Challis–Kamloops belt of south central British Columbia. Journal of Volcanology and Geothermal Research 126, 303–326.

Drummond, M.S., Defant, M.J., 1990. A model for trondhjemite–tonalite–dacite genesis and crustal growth via slab melting; archean to modern comparisons. Journal of Geophysical Research 95, 21,503–21,521.

Drummond, M.S., Defant, M.J., Kepezhinskas, P.K., 1996. Petrogenesis of slab-derived trondhjemite–tonalite–dacite/adakite magmas. In: Brown, M., Candela, P.A., Pecket, D.L. (Eds.), The Third Hutton Symposium on the Origin of Granites and Related Rocks, Special Paper, vol. 315. Geological Society of America, Boulder, CO, pp. 205–215.

Forsythe, R., Nelson, E., 1985. Geological manifestations of ridge collision; evidence from the Golfo de Penas–Taitao basin, southern Chile. Tectonics 4, 477–495.

Frederiksen, A.W., Bostock, M.G., VanDecar, J.C., Cassidy, J.F., 1998. Seismic structure of the upper mantle beneath the northern Canadian Cordillera from teleseismic travel-time inversion. Tectonophysics 294, 43–55.

Garrison, J.M., Davidson, J.P., 2003. Dubious case for slab melting in the northern volcanic zone of the Andes. Geology 31, 565–568.

Gill, J.B., 1981. Orogenic Andesites and Plate Tectonics. Springer-Verlag, Berlin.

Gorring, M.L., Kay, S.M., Zeitler, P.K., Ramos, V.A., Rubiolo, D., Fernandez, M.L., Panza, J.L., 1997. Neogene Patagonian plateau lavas; continental magmas associated with ridge collision at the Chile triple junction. Tectonics 16, 1–17.

Green, T.H., 1982. Anatexis of mafic crust and high pressure crystallization of andesite. In: Thorpe, R.S. (Ed.), Andesites; Orogenic Andesites and Related Rocks. John Wiley & Sons, Chichester, UK, pp. 465–487.

Green, N.L., 1994. Mount St. Helens; potential example of the partial melting of the subducted lithosphere in a volcanic arc; discussion. Geology 22, 188–189.

Green, N.L., Harry, D.L., 1999. On the relationship between subducted slab age and arc basalt petrogenesis, Cascadia subduction system, North America. Earth and Planetary Science Letters 171, 367–381.

Groome, W.G., Thorkelson, D.J., Friedman, R.M., Mortensen, J.K., Massey, N.W.D., Marshall, D.D., Layer, P.W., 2003. Magmatic and tectonic history of the leech river complex, Vancouver island, British Columbia: evidence for ridge–trench intersection and accretion of the crescent terrane. In: Sisson, V.B., Roeske, S., Pavlis, T.L. (Eds.), Geology of a Transpressional Orogen Developed During Ridge–Trench Interaction Along the North Pacific Margin, Special Paper, vol. 371. Geological Society of America, Boulder, CO, pp. 327–354.

Haeussler, P.J., Bradley, D.C., Goldfarb, R.J., Snee, L.W., Taylor, C.D., 1995. Link between ridge subduction and gold mineralization in southern Alaska. Geology 23, 995–998.

Haeussler, P.J., Bradley, D.C., Wells, R.E., Miller, M.L., 2003. Life and death of the resurrection plate: evidence for its existence and subduction in the northeastern pacific in Paleocene–Eocene time. Geological Society of America Bulletin 115, 867–880.

Harry, D.L., Green, N.L., 1999. Slab dehydration and basalt petrogenesis in subduction systems involving very young oceanic lithosphere. Chemical Geology 160, 309–333.

Hole, M.J., Larter, R.D., 1993. Trench-proximal volcanism following ridge crest–trench collision along the Antarctic Peninsula. Tectonics 12, 879–910.

Hole, M.J., Rogers, G., Saunders, A.D., Storey, M., 1991. Relation between alkalic volcanism and slab-window formation. Geology 19, 657–660.

Iwamori, H., 2000. Thermal effects of ridge subduction and its implications for the origin of granitic batholith and paired metamorphic belts. Earth and Planetary Science Letters 181, 131–144.

Johnson, C.M., O'Neil, J.R., 1984. Triple junction magmatism; a geochemical study of Neogene volcanic rocks in western California. Earth and Planetary Science Letters 71, 241–263.

Johnston, S.T., Thorkelson, D.J., 1997. Cocos-Nazca slab window beneath central America. Earth and Planetary Science Letters 146, 465–474.

Kay, R.W., 1978. Aleutian magnesian andesites; melts from subducted Pacific Ocean crust. Journal of Volcanology and Geothermal Research 4, 117–132.

Kay, S.M., Ramos, V.A., Marquez, M., 1993. Evidence in Cerro Pampa volcanic rocks for slab-melting prior to ridge–trench collision in southern south America. Journal of Geology 101, 703–714.

Kepezhinskas, P., McDermott, F., Defant, M.J., Hochstaedter, A., Drummond, M.S., Hawkesworth, C.J., Koloskov, A., Maury, R.C., Bellon, H., 1997. Trace element and Sr–Nd–Pb isotopic constraints on a three-component model of Kamchatka arc petrogenesis. Geochimica et Cosmochimica Acta 61, 577–600.

Lewis, T.J., Lowe, C., Hamilton, T.S., 1997. Continental signature of a ridge–trench–triple junction; northern Vancouver island. Journal of Geophysical Research 102, 7767–7781.

Lopez, S., Castro, A., 2001. Determination of the fluid-absent solidus and supersolidus phase relationships of MORB-derived amphibolites in the range 4–14 kbar. American Mineralogist 86, 1396–1403.

Marshak, R.S., Karig, D.E., 1977. Triple junctions as a cause for anomalously near-trench igneous activity between the trench and volcanic arc. Geology 5, 233–236.

Maury, R.C., Sajona, F.G., Pubellier, M., Bellon, H., Defant, M.J., 1996. Fusion de la croûte océanique dans les zones de subduction/collision récentes; l'exemple de Mindanao (Philippines). Bulletin de la Societe Geologique de France 167, 579–595.

Murdie, R.E., Russo, R.M., 1999. Seismic anisotropy in the region of the Chile margin triple junction. Journal of South American Earth Sciences 12, 261–270.

Peacock, S.M., 1993. Large-scale hydration of the lithosphere above subducting slabs. Chemical Geology 108, 49–59.

Peacock, S.M., 1996. Thermal and petrologic structure of subduction zones (overview). In: Bebout, G.E., Scholl, D.W., Kirby, S.H., Platt, J.P. (Eds.), Subduction Top to Bottom, Geophysical Monograph, vol. 96. American Geophysical Union, Washington, DC, pp. 119–133.

Peacock, S.M., Rushmer, T., Thompson, A.B., 1994. Partial melting of subducting oceanic crust. Earth and Planetary Science Letters 121, 227–244.

Rapp, R.P., Shimizu, N., Norman, M.D., Applegate, G.S., 1999. Reaction between slab-derived melts and peridotite in the mantle wedge; experimental constraints at 3.8 GPa. Chemical Geology 160, 335–356.

Rogers, G., Saunders, A.D., 1989. Magnesian andesites from Mexico, Chile and the Aleutian islands; implications for magmatism associated with ridge–trench collision. In: Crawford, A.J. (Ed.), Boninites. Unwin Hyman, London, UK, pp. 416–445.

Ruff, L.J., Tichelaar, B.W., 1996. What controls the seismogenic plate interface in subduction zones? In: Bebout, G.E., Scholl, D.W., Kirby, S.H., Platt, J.P. (Eds.), Subduction Top to Bottom, Geophysical Monograph, vol. 96. American Geophysical Union, Washington, DC, pp. 105–111.

Saunders, A.D., Norry, M.J., Tarney, J., 1988. Origin of MORB and chemically-depleted mantle reservoirs; trace element constraints. Oceanic and Continental Lithosphere; Similarities and Differences, Journal of Petrology Special Issue, pp. 415–445.

Saunders, A.D., Norry, M.J., Tarney, J., 1991. Fluid influence on the trace element compositions of subduction zone magmas. Philosophical Transactions of the Royal Society of London. Series A 335, 377–392.

Severinghaus, J., Atwater, T., 1990. Cenozoic geometry and thermal state of the subducting slabs beneath western north America. In: Wernicke, Brian, P. (Eds.), Basin and Range Extensional Tectonics Near the Latitude of Las Vegas, Nevada, Memoir, vol. 176. Geological Society of America, Boulder, CO, pp. 1–22.

Sisson, V.B., Pavlis, T.L., 1993. Geological consequences of plate reorganization: an example from the Eocene southern Alaskan fore arc. Geology 21, 913–916.

Sisson, V.B., Pavlis, T.L., Prior, D.J., 1994. Penrose conference report; effects of triple junction interactions at convergent plate margins. GSA Today 4, 248–249.

Sisson, V.B., Pavlis, T.L., Roeske, S.M., Thorkelson, D.J., 2003. An overview of ridge–trench interactions in modern and ancient settings. In: Sisson, V.B., Roeske, S., Pavlis, T.L. (Eds.), Geology of a Transpressional Orogen Developed During Ridge–Trench Interaction Along the North Pacific Margin, Special Paper, vol. 371. Geological Society of America, Boulder, CO, pp. 1–18.

Sleep, N.H., Ebinger, C.J., Kendall, J.M., 2002. Deflection of mantle plume material by cratonic keels. In: Fowler, C.M.R., Ebinger, C.J., Hawkesworth, C.J. (Eds.), The Early Earth; Physical,

Chemical and Biological Development, Special Publication, vol. 199. Geological Society, London, UK, pp. 135–150.
Stein, S., Stein, C.A., 1996. Thermo-mechanical evolution of the oceanic lithosphere: implications for the subduction process and deep earthquakes. In: Bebout, G.E., Scholl, D.W., Kirby, S.H., Platt, J.P. (Eds.), Subduction Top to Bottom, Geophysical Monograph, vol. 96. American Geophysical Union, Washington, DC, pp. 1–17.
Tatsumi, Y., 1989. Migration of fluid phases and genesis of basalt magmas in subduction zones. Journal of Geophysical Research 94, 4697–4707.
Thompson, A.B., Ellis, D.J., 1994. $CaO+MgO+Al_2O_3+SiO_2+H_2O$ to 35 kb; amphibole, talc, and zoisite dehydration and melting reactions in the silica-excess part of the system and their possible significance in subduction zones, amphibolite melting, and magma fractionation. American Journal of Science 10, 1229–1289.
Thorkelson, D.J., 1996. Subduction of diverging plates and the principles of slab window formation. Tectonophysics 255, 47–63.
Thorkelson, D.J., Taylor, R.P., 1989. Cordilleran slab windows. Geology 17, 833–836.
van Keken, P.E., Kiefer, B., Peacock, S.M., 2002. High-resolution model of subduction zones: implications for mineral dehydration reactions and the transport of water into the deep mantle. Geochemistry, Geophysics, Geosystems 3, 1–20.
Wyllie, P.J., 1984. Sources of granitoid magmas at convergent plate boundaries. Physics of the Earth and Planetary Interiors 35, 12–18.